

Photoisomerization of a sterically constrained merocyanine dye

Andrew C. Benniston^a and Anthony Harriman^b

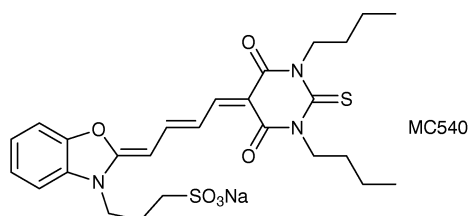
^a Chemistry Department, University of Glasgow, Glasgow, UK G12 8QQ

^b Laboratoire de Photochimie, Ecole de Chimie, Polymères et Matériaux, Université Louis Pasteur, 1 rue Blaise Pascal, F-67008 Strasbourg, France

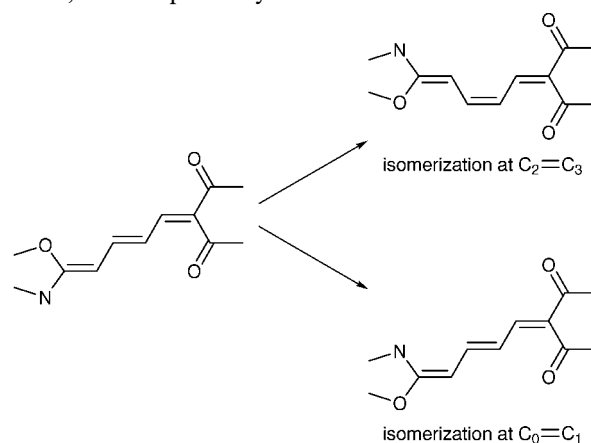
A particular concern regarding the photophysical properties of merocyanine 540 derivatives, and related cyanine dyes, involves identifying which double bond in the central polyenic bridge undergoes light-induced isomerization. In order to address this issue we have synthesized a novel merocyanine dye in which the first double bond is built into a cyclic structure that prevents isomerization at this site. Contrary to expectations, the dye photoisomerizes with reasonable efficiency, such that the quantum yields of fluorescence and intersystem crossing to the triplet manifold are kept small. For this dye, isomerization must take place at the central double bond. It is further shown that the strategy of inserting bulky or constraining groups into the polyenic bridge is not a viable approach for the development of highly fluorescent merocyanine dyes.

Certain merocyanine dyes are able to recognize leukemia cells and to assimilate selectively into infected cells, even in the presence of a large excess of healthy cells.¹ *In situ* dye is both fluorescent, thereby permitting facile detection of labelled cells, and photoactive, hence providing for destruction of labelled cells under visible light illumination.² Unfortunately, the photophysical properties of the prototypic merocyanine dye, Merocyanine 540 (MC540), are inconducive^{3–7} for its application in either diagnosis or therapy and numerous derivatives have been developed^{8–11} in order to improve this position. The poor photophysical properties arise because the central polyenic bridge undergoes rapid photoisomerization¹² from the original *trans*-configuration into a long-lived *cis*-isomer. This process is competitive with fluorescence and intersystem crossing to such an extent that it dominates the photophysical properties of MC540.¹³ We have tried various approaches to overcome the effects of rapid photoisomerization, in some cases with considerable success, and a useful strategy for the development of highly photoactive forms of MC540 has evolved.^{8–11} Identification of fluorescent dyes suitable for the early recognition of leukemia has been less successful and, to date, we have failed to produce a class of dyes displaying exceptionally high specificity for infected cells.¹ It has also proved difficult to develop merocyanine dyes that are highly fluorescent but not photoactive, and thus could be used for the quantitative estimation of infected cells at very low levels of contamination. Some progress has been made in this latter area in that dyes are now available that are more resistant to self-sensitized photobleaching.¹⁴

A crucial issue concerns identifying which of the three double bonds in the central polyenic bridge is the most susceptible to photoisomerization. Note that in all cases studied, the ground state exists unequivocally in the all-*trans* alignment. We can eliminate the double bond adjacent to the thiobarbiturate unit, since rotation at this site would not produce a spectroscopically distinct isomer. In addition, the thiobarbiturate is locked in place *via* internal hydrogen bonding¹⁵ and it has been shown that varying the length of alkyl groups



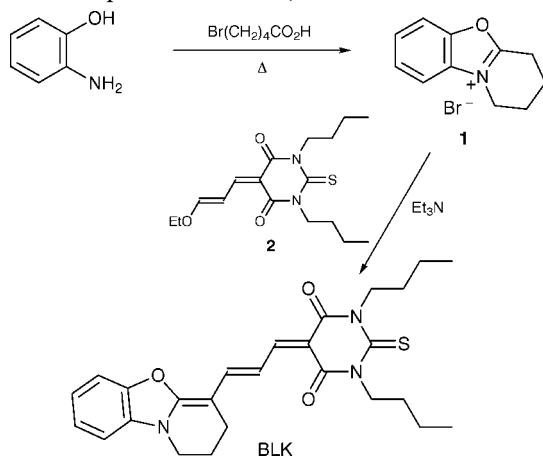
attached to the N atoms in the thiobarbiturate has only a small effect on the rate of isomerization.⁹ There seems no obvious reason why isomerization should take place preferentially at the central double bond rather than at the double bond closest to the benzoxazole, since this would involve rotation of a larger volume. Moreover, attaching bulky groups at the first carbon atom in the polyene backbone (C₁) has little effect on the rate of isomerization,¹¹ leading to the suggestion that the first double bond is the more easily rotated. Constraining the central double bond into a six-membered ring prevents formation of the *cis*-isomer, possibly indicating that isomerization occurs at the central double bond but, for this molecule, steric crowding also inhibits isomerization around the first double bond.¹¹ The temptation, therefore, is to accept that isomerization takes place at the C₀=C₁ double bond, since this is consistent with all the experimental data, and we have sought confirmation of this assumption. In so doing we have attempted to design a new class of merocyanine dyes for which isomerization is prevented by stereochemical constraints and which, therefore, will be unusually fluorescent. This possibility is explored herein by comparing the photophysical properties of a novel merocyanine dye, BLK, in which isomerization at the C₀=C₁ double bond is constrained, with the parent dye.



Experimental Materials

Merocyanine 540 MC540 was obtained from Eastman-Kodak and was purified by column chromatography on silica using acetone–methanol 98/2 as eluant; the absorption maximum

(λ_{MAX}) in dilute ethanol solution was located at 560 nm with a molar absorption coefficient (ϵ_{MAX}) of $187\,000\text{ dm}^3\text{ mol}^{-1}\text{ cm}^{-1}$. The basic methodology used for preparation of the new dye BLK is shown below in Scheme 1 and follows our strategy developed earlier for the synthesis of related merocyanine dyes.^{8–11} Raw materials were purchased from Aldrich Chemicals or Eastman-Kodak and were used as received. Ethanol (Aaper, Absolute grade) was used as received. All other solvents were spectroscopic grade, used as received, or redistilled under vacuum. Silica gel (40–60 mesh) was purchased from Phase Separation Limited. Compounds **1**¹⁶ and **2**¹¹ were prepared according to the literature, the former by a slight modification of the published method, as described below.



Scheme 1

Preparation of **1**

2-Aminophenol (3 g, 27.5 mmol) and 5-bromo-2-pyrrolidone (7.5 g, 27.5 mmol) were heated together at 170°C for 2 h before raising the temperature to 190°C for 5 min (note: overheating the mixture caused considerable charring, difficulty in purification, and a decrease in yield). After cooling the reaction mixture to room temperature, the resultant solid was triturated with dry acetone, removed by filtration and washed successively with acetone (10 cm^3) and diethyl ether (10 cm^3). The solid was dried under vacuum. Yield 4.3 g, 63%. ^1H NMR ($[\text{D}_6\text{-}]\text{acetone}$): $\delta = 2.33\text{--}2.41$ (m, 4H); $3.54\text{--}3.60$ (t, 2H, $J = 5.0$ Hz); $4.62\text{--}4.67$ (t, 2H, $J = 4.5$ Hz); $7.73\text{--}7.80$ (m, 2H); $8.00\text{--}8.11$ (m, 2H). MS (EI): $m/z = 173$ ($\text{M}-\text{HBr}$)⁺. IR (KBr disc) $\nu = 1604\text{ cm}^{-1}$ (C=N).

Preparation of BLK

Compounds **1** (38 mg, 0.15 mmol) and **2** (50 mg, 0.15 mmol) were refluxed overnight in methanol (20 cm^3) containing a few drops of triethylamine. During this time the colour of the solution changed from red to deep purple. The solvent was removed on a rotary evaporator and the crude mixture was passed down a silica-gel column, eluting with ethyl acetate to remove impurities, followed by acetone to afford a still slightly contaminated product. A second chromatographic separation on silica gel, eluting with a chloroform–acetone mixture (50:50), afforded a purple solid which was recrystallised from acetone. Yield 69 mg, 40%. ^1H NMR (CDCl_3): $0.94\text{--}0.98$ (t, 6H, $J = 7.2$ Hz); $1.39\text{--}1.43$ (m, 4H); 1.72 (m, 4H); 2.23 (m, 2H); 2.83 (m, 2H); 4.08 (m, 2H); 4.46 (m, 4H); $7.15\text{--}7.17$ (d, 1H, $J = 7.2$ Hz); $7.33\text{--}7.38$ (m, 2H); $7.48\text{--}7.50$ (d, 1H, $J = 7.6$ Hz); $7.67\text{--}7.75$ (t, 1H, $J = 13.2$ Hz); $7.79\text{--}7.83$ (d, 1H, $J = 13.1$ Hz); $7.94\text{--}7.98$ (d, 1H, $J = 12.9$ Hz). MS (EI): $m/z = 465$ (M)⁺. UV–VIS ($\text{C}_2\text{H}_5\text{OH}$): $\lambda_{\text{MAX}} = 561\text{ nm}$ ($\epsilon_{\text{MAX}} = 77\,000\text{ dm}^3\text{ mol}^{-1}\text{ cm}^{-1}$).

Methods

^1H NMR spectra were recorded with a Bruker AM360 FT-NMR instrument with TMS as internal standard. Absorp-

tion spectra were recorded with a Uvikon 930 spectrophotometer and fluorescence spectra were recorded with a fully corrected Perkin-Elmer LS50 spectrofluorimeter. Solutions for fluorescence studies were adjusted to possess an absorbance of <0.05 at the excitation wavelength. Singlet excited-state lifetimes were measured with a Hamamatsu single-shot streak camera following excitation by a 30 ps laser pulse at 532 nm. A narrow bandpass filter was used to isolate fluorescence over the spectral range (600 ± 10) nm and the laser intensity was attenuated so as not to saturate the streak camera. Approximately 100 individual laser shots were averaged and the laser profile was deconvoluted from the experimental decay record prior to data analysis. The time window of the streak camera was 50 ps to 10 ns.

Flash spectrographic studies were made with a frequency-doubled, Q-switched Nd:YAG laser (pulse width 20 ns; pulse energy 250 mJ). Solutions were adjusted to possess an absorbance of *ca.* 0.2 at 532 nm and were purged with N_2 or air, according to the needs of the experiment. Transient differential absorption spectra were recorded point-by-point while kinetic studies were made at fixed wavelength with the data being analysed by non-linear, least-squares iterative procedures. The laser intensity was attenuated, as necessary, with metal screen filters. In several cases it was necessary to restrict the intensity of the monitoring beam to a low level in order to avoid photolysis of the photoisomer. Such attenuation was achieved by placing appropriate neutral density filters before the sample cell.

Differential molar absorption coefficients for the triplet excited state were measured by the energy-transfer method, using anthracene as donor. A solution of anthracene in ethanol was prepared so as to possess an absorbance of 0.3 at 355 nm and deoxygenated by purging with N_2 . The triplet absorption signal was monitored at the peak¹⁷ of 422 nm and the laser intensity was attenuated until the decay profile could be fit to a single-exponential process. Various concentrations of BLK were added to the solution and the lifetime of triplet anthracene was measured at 422 nm. For each solution, the rate of formation of the triplet state of the merocyanine dye was monitored at 680 nm and compared with the rate of decay of triplet anthracene. The concentration of BLK was increased until the dye began to compete with anthracene for absorption of the excitation laser pulse. At moderately high dye concentrations, triplet energy transfer was quantitative (*i.e.* decay and formation rates were similar within experimental error) and the concentration of dye triplet was determined by reference to triplet anthracene possessing a differential extinction coefficient¹⁸ at 422 nm of $52\,000\text{ dm}^3\text{ mol}^{-1}\text{ cm}^{-1}$. The averaged molar absorption coefficient at 680 nm was $(40\,000 \pm 6000)\text{ dm}^3\text{ mol}^{-1}\text{ cm}^{-1}$.

Differential molar absorption coefficients for the *cis*-isomer formed under illumination were determined by the previously described¹¹ complete conversion method, in aerated ethanol. A dilute solution of BLK was prepared to possess an absorbance at the peak maximum of *ca.* 0.10 and irradiated with a single pulse delivered from a mode-locked Nd:YAG pumped dye laser (40 mJ, 200 ps). The excitation wavelength was 560 nm, while the monitoring beam was passed through a high-radiance monochromator also tuned to 560 nm. The laser intensity was varied with crossed-polarizers and the differential absorption signal due to conversion of the ground-state species into the unstable isomer was measured. The photomultiplier tube was protected from scattered laser light with an optical shutter that was opened 10 ns after the excitation pulse. Approximately 100 individual laser shots were averaged and the decay profile extrapolated to zero time. The laser intensity was calibrated using zinc *meso*-tetraphenylporphyrin in benzene as standard.^{19,20} The size of the bleaching signal increased with increasing laser intensity before reaching an optimum value, after which the signal began to decrease with

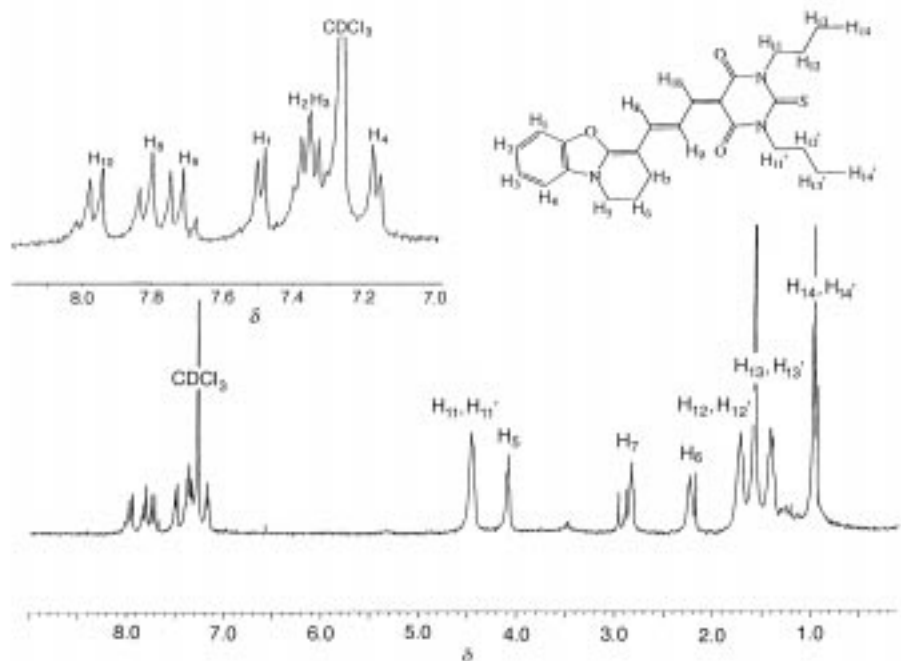


Fig. 1 360 MHz ^1H NMR spectrum of the novel constrained dye BLK in CDCl_3 showing the atomic labelling. The inset shows an expansion of the aromatic region.

increasing laser power. This latter effect arises because the *cis*-isomer is photolabile and absorbs the incident laser pulse. The experimental conditions were optimized so as to minimize the significance of this effect and extinction coefficients were calculated from the maximum bleaching signal.

Computational studies were made on a VAX workstation. Structures of BLK were drawn and minimized using MM2 molecular mechanics simulations. The structures were subsequently refined using MOPAC version 94.10. Molecular orbital (MO) calculations were made for the minimized conformations using AM1 parameters to estimate bond lengths and valence electronic charges on selected carbon atoms in the polyenic backbone. The bond order at the isomerizing bond (N_{BO}) was calculated from the computed bond length (D) using the expression derived by Pauling²¹

$$D = D_1 - 0.70 \log N_{\text{BO}} \quad (1)$$

where D_1 is the expected bond length ($D_1 = 1.504 \text{ \AA}$) for a C—C single bond in a structure that has several equivalent resonance forms.

Results and Discussion

Ground-state conformation of BLK

The 360 MHz ^1H NMR spectrum of the new dye BLK in CDCl_3 at ambient temperature is shown in Fig. 1 and is similar in appearance to spectra obtained for non-constrained merocyanine derivatives.^{9,11} In the downfield region, three alkenic signals (two doublets and a triplet) were unequivocally assigned by way of their characteristic coupling constants. The most downfield peak ($\delta = 7.9$, $J = 12.9 \text{ Hz}$) is assigned to H_{10} since the zwitterionic resonance contribution diminishes the electron density at this methine carbon. The second doublet ($\delta = 7.8$, $J = 13.1 \text{ Hz}$) is accordingly assigned to the proton marked H_8 , with the triplet resonance ($\delta = 7.7$, $J = 13.2 \text{ Hz}$) being necessarily due to the central proton H_9 . The ^1H NMR spectrum, however, does not indicate the geometrical structure of the molecule and such information became clear only from a series of nuclear Overhauser enhancement (NOE) experiments.

Selected NOE difference spectra are displayed in Fig. 2. The proton H_5 was identified by its characteristic chemical shift ($\delta = 4.08$) and by its positive NOE on the aromatic proton H_4 of the benzoxazole group [Fig. 2(ii)]. There is an accompanying positive NOE at $\delta = 2.2$ which can be assigned, unambiguously, to H_6 of the constraining propyl group. Although not shown, the difference spectrum obtained upon irradiation of resonance H_6 confirmed the peak located at $\delta = 2.8$ as being due to H_7 . In Fig. 2(i) is depicted the NOE difference spectrum obtained upon irradiation of the resonance marked

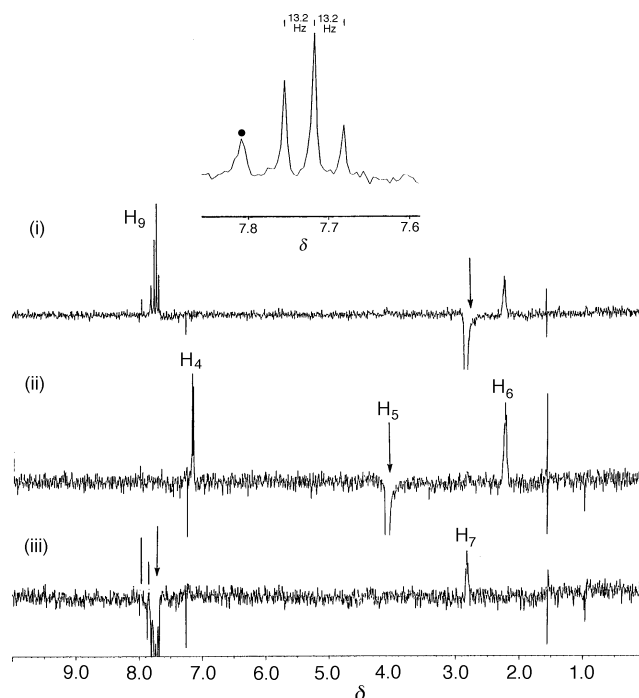


Fig. 2 Series of NOE difference spectra recorded for BLK in CDCl_3 confirming the all-*trans* arrangement of the polymethine backbone. The irradiation point for each experiment is indicated by a dark arrow. The inset shows an expanded view of the resonance assigned to H_9 indicating the triplet coupling constants and the weak NOE to H_8 denoted with (●).

H₇. The spectrum clearly shows an enhanced resonance that appears as a triplet centred at $\delta = 7.7$ with a coupling constant of 13.2 Hz accompanied by a smaller broad peak located at $\delta = 7.8$. The smaller resonance at $\delta = 7.8$ is presumably a weaker NOE of the opposite H₈ proton whereas the spectrum [Fig. 2(iii)] obtained from selective irradiation of the resonance H₉ displayed only an NOE with resonance H₇.

These various results provide firm support for the assignment of an all-*trans* alignment of the polyenic backbone in BLK. Furthermore, close examination of the ¹H NMR spectra recorded in CDCl₃ shows that only a single isomer is present, at least within the observable limit (*i.e.* ca. 95%) of NMR spectroscopy. The same conclusions have been reached previously for MC540¹⁵ and several related merocyanine dyes^{9,10} and it is clear that the constraining propyl chain does not cause a substantial modification of the ground-state structure. Note, however, that this is the first time it has been possible to establish that the N atom of the benzoxazole unit lies *trans* to the polyene bridge. This structure was inferred earlier on the basis of MO calculations made for a variety of MC540 derivatives.¹¹ Identical MO calculations made for BLK indicate that the *trans*-isomer is more stable than the corresponding *cis*-isomer by ca. 75 kJ mol⁻¹ (Fig. 3). These calculations also indicate steric interaction between the propyl constraining chain and the polyenic bridge, especially the proton at H₉. This introduces slight distortion into the molecular backbone, with respect to the unconstrained MC540, causing minor deviation from planarity. Thus, the torsion angle around the N—C₀—C₁—C₂ axis is higher for BLK ($\theta \approx 2.2^\circ$) than for MC540 ($\theta \approx 1.1^\circ$).

Photophysical properties of BLK in ethanol

The absorption spectrum recorded for BLK in dilute ethanol solution (Fig. 4) shows an intense band centred at 561 nm for which the peak maximum (λ_{MAX}) is also the (0,0) transition. The molar absorption coefficient measured at the peak maximum ($\epsilon_{\text{MAX}} = 77\,000 \pm 7\,000 \text{ dm}^3 \text{ mol}^{-1} \text{ cm}^{-1}$) is reduced almost two-fold with respect to the parent dye (Table 1) and the absorption profile is relatively broad. The oscillator

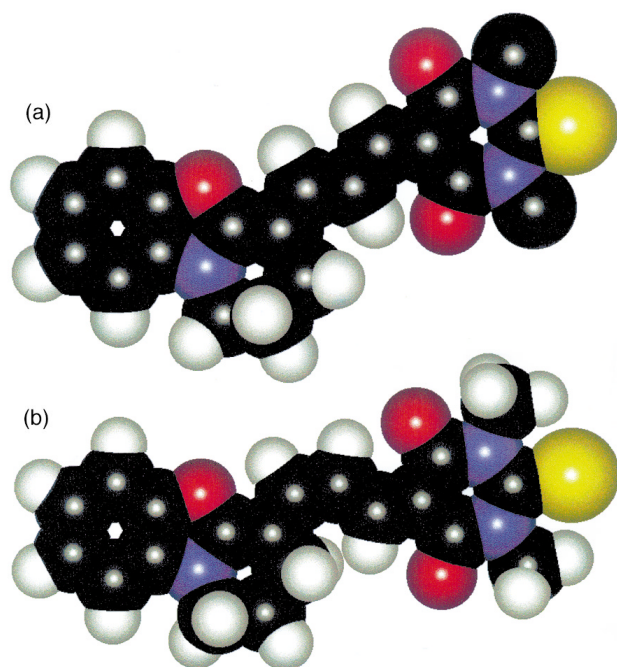


Fig. 3 Space-filling representations of the MM2 calculated (energy minimized) structures of the (a) *trans*- and (b) *cis*-isomer of BLK. Sulfur is shown in yellow, nitrogen in blue, oxygen in red, hydrogen in white, and carbon in black. Note that the *n*-butyl chains attached to the N atoms of the thiobarbiturate unit are represented as methyl groups for clarity of presentation.

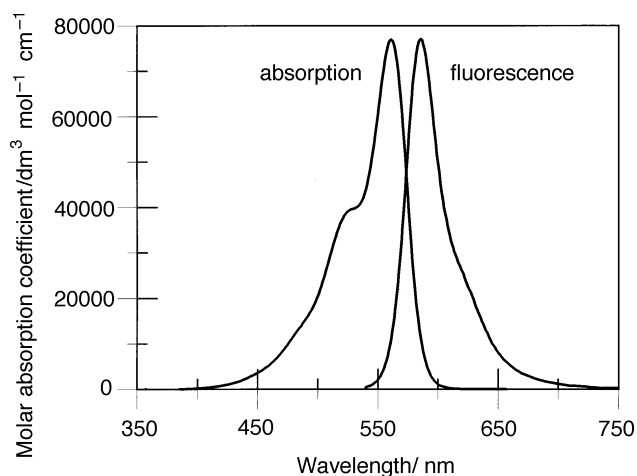


Fig. 4 Absorption and fluorescence spectra recorded for BLK in dilute ethanol solution. The excitation wavelength used for the fluorescence spectrum was 540 nm.

strength (f) for the transition calculated according to²²

$$f = \frac{4.39 \times 10^{-9}}{n} \int \epsilon(\nu) d\nu \quad (2)$$

where $\epsilon(\nu)$ refers to the molar absorption coefficient at wavenumber ν (in cm⁻¹) and n is the refractive index of the surrounding solvent ($f = 0.58$) is much smaller than that determined for MC540 ($f = 0.88$). The absorption profile, which follows Beer's law over the concentration range used here, and which closely matches the fluorescence excitation spectrum, can be deconvoluted into a series of four Gaussian-shaped bands having an average spacing of 1100 cm⁻¹ and a half-width of 1010 cm⁻¹. These values are reasonable, considering the relatively narrow band shape of the absorption profile. The spectrum contains no indication of an underlying broad transition that might be due to a dimer,²³ while the spectral curve-fitting routine does not require overlapping of two slightly split spectral profiles. The latter situation would

Table 1 Comparison of the properties measured for the constrained dye BLK and the unconstrained parent MC540 in deoxygenated ethanol solution

property	MC540	BLK
$\lambda_{\text{max}}/\text{nm}^a$	560	561
$\epsilon_{\text{max}}/\text{dm}^3 \text{ mol}^{-1} \text{ cm}^{-1}^a$	187 000	77 000
f^c	0.88	0.58
Φ_F^d	0.16	0.11
τ_S/ps^e	410	480
$k_F/10^8 \text{ s}^{-1f}$	4.8	2.3
Φ_T^g	0.0030	0.0042
$\tau_T/\mu\text{s}^h$	800	560
Φ_I^i	0.40	0.02
τ_I/ms^j	6.8	10.6
$k_{IC}/10^8 \text{ s}^{-1k}$	20.5	18.5
$k_{TC}/10^8 \text{ s}^{-1l}$	9.8	0.42
$\mu_{\text{GS}}/\text{D}^m$	13.2	15.0
$\mu_{\text{SS}}/\text{D}^n$	14.0	14.6
V_{EC}^o	4.297(4.254)	4.298(4.303)
N_{BO}^p	1.58(1.60)	1.63

^a Absorption maximum, ± 1 nm; ^b molar absorption coefficient, $\pm 6\%$; ^c oscillator strength calculated from eqn. (2), ± 0.02 ; ^d fluorescence quantum yield, $\pm 8\%$; ^e excited-singlet-state lifetime, ± 20 ps; ^f radiative rate constant calculated from eqn. (3), $\pm 10\%$; ^g triplet quantum yield, $\pm 25\%$; ^h triplet lifetime, ± 50 μs ; ⁱ quantum yield for formation of the *cis*-isomer, $\pm 20\%$; ^j lifetime of the *cis*-isomer, ± 0.1 ms; ^k rate constant for internal conversion, $\pm 10\%$; ^l rate constant for formation of the *cis*-isomer, $\pm 20\%$; ^m calculated dipole moment of the ground state, ± 0.2 D; ⁿ calculated dipole moment of the excited singlet state, ± 0.2 D; ^o calculated valence electronic charge at C₁(C₃), ± 0.002 ; ^p calculated bond order at the isomerizing bond (at the C₂=C₃ bond), ± 0.2 .

arise if the sample comprised a mixture of two isomers, although this was not apparent from the ^1H NMR spectroscopic studies. Instead, it appears that the spectral broadening is a consequence of the small extent of structural distortion imposed by the constraining propyl chain.

Fluorescence is readily detected following excitation into the lowest-energy absorption transition (Fig. 4), with the fluorescence excitation spectrum giving a good match to the absorption profile over the entire visible spectral range. The fluorescence profile shows relatively poor mirror symmetry with respect to the absorption spectrum and, in particular, appears to be narrower, despite the larger slit widths used with the spectrofluorimeter. As found for other merocyanine derivatives, the slight vibronic shoulder is not observed in the fluorescence profile.¹¹ Spectral curve fitting showed that the fluorescence spectrum could be reproduced by a series of four Gaussian-shaped bands having an average spacing of 1000 cm^{-1} and a half-width of 850 cm^{-1} . Such analysis confirms the idea that the absorption profile is unusually broad for a merocyanine dye, while the fluorescence profile remains similar to that of the unconstrained MC540. The Stokes shift,²² measured in dilute ethanol solution, was $(1780 \pm 100)\text{ cm}^{-1}$, which is *ca.* three-fold larger than that found for MC540 under identical conditions. Taken together these various results are indicative of a modest structural change upon promotion to the first-excited singlet state.

The absorption and fluorescence maxima undergo substantial blue shifts as the solvent polarity is increased, but without modification of the respective spectral profiles. Within experimental limits, the magnitude of the Stokes shift is insensitive to changes in solvent polarity. Thus, BLK is a relatively polar merocyanine dye,¹⁴ for which the dipole moment is not changed significantly upon population of the first excited-singlet state. Internal polarity arises because of the involvement of zwitterionic resonance forms in which the N atom of the benzoxazole unit functions as the primary electron donor and the carbonyl groups of the thiobarbiturate unit represent the primary electron acceptors. It is interesting to note that the presence of a constraining propyl chain does not inhibit zwitterion formation but, on the contrary, BLK seems to be slightly more polar than MC540. This is apparent both from the effect of polar solvents on the absorption and fluorescence spectral maxima and from MO calculations made with AM1 parameters. In the latter case, the dipole moment (μ) calculated for the ground state of BLK was estimated as 15.0 D compared to a value of $\mu = 13.2\text{ D}$ calculated for the ground state of MC540. The calculations indicate that there is no real change in polarity upon promotion to the first excited-singlet state of BLK ($\mu = 14.6\text{ D}$).

The fluorescence quantum yield (Φ_{F}), measured relative to Rhodamine 101 in ethanol,²⁴ was found to be (0.11 ± 0.01) while the fluorescence lifetime (τ_{F}) was measured to be $(480 \pm 30)\text{ ps}$ in dilute ethanol solution at 20°C . The fluorescence decay profile was strictly single exponential, regardless of detection wavelength, and the measured lifetime was unaf-

ected by the presence of dissolved oxygen. The radiative rate constant was calculated from the Strickler–Berg expression²⁵

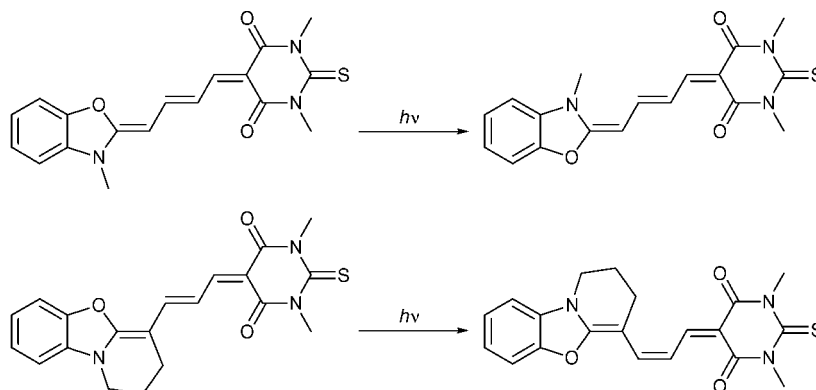
$$k_{\text{F}} = 2.88 \times 10^{-9} n^2 \frac{\int F(\nu) d\nu}{\int \frac{F(\nu)}{\nu^3} d\nu} \int \frac{\epsilon(\nu)}{\nu} d\nu \quad (3)$$

where $F(\nu)$ is the fluorescence intensity at wavenumber ν . The derived value ($k_{\text{F}} = 2.3 \times 10^8\text{ s}^{-1}$) was found to be in excellent agreement with that estimated from the experiment data ($k_{\text{F}} = \Phi_{\text{F}}/\tau_{\text{F}}$).

Laser flash photolysis studies carried out in N_2 -saturated ethanol solution indicate that there are two transient species present after decay of the first excited-singlet state [Fig. 5(a) and (b)]. The shorter-lived transient, which absorbs predominantly around 700 nm, is assigned to the triplet excited state of the dye, on account of its reactivity towards molecular oxygen. The longer-lived transient, which absorbs weakly at 580 nm [Fig. 5(c)], did not react with oxygen and, on the basis of related studies made with various merocyanine dyes,^{2–11} this species is believed to be a geometric isomer formed by rotation around one of the double bonds in the polyene backbone. Under low illumination conditions, the lifetime of the isomer (τ_{I}) was $(10.6 \pm 0.1)\text{ ms}$, with decay following first-order kinetics and restoring the pre-pulse baseline. The differential molar absorption coefficient for the isomer at 580 nm was derived to be $(8000 \pm 1250)\text{ dm}^3\text{ mol}^{-1}\text{ cm}^{-1}$, as measured by complete conversion. Using this value, the quantum yield for formation of the isomer (Φ_{I}) was found to be (0.02 ± 0.004) following excitation with a 200 ps laser pulse.

The triplet state decayed with a lifetime (τ_{T}) of $(560 \pm 50)\text{ ps}$ in deaerated ethanol and was quenched by O_2 with a bimolecular rate constant of $(1.3 \pm 0.3) \times 10^9\text{ dm}^3\text{ mol}^{-1}\text{ s}^{-1}$. The triplet state could also be populated *via* energy transfer from triplet anthracene in ethanol following laser excitation at 355 nm [Fig. 5(d)]. From these studies, the bimolecular rate constant for triplet energy transfer was found to be $(4 \pm 1) \times 10^9\text{ dm}^3\text{ mol}^{-1}\text{ s}^{-1}$ and the differential molar absorption coefficient for the triplet at the peak of 680 nm was $(40\,000 \pm 6000)\text{ dm}^3\text{ mol}^{-1}\text{ s}^{-1}$. On the basis of actinometric laser flash photolysis studies made with a 200 ps laser pulse, the quantum yield for population of the triplet excited state (Φ_{T}) was determined to be (0.0042 ± 0.0011) .

The photophysical properties recorded for the new merocyanine dye BLK are compared with those measured under identical conditions for the parent dye MC540 in Table 1. The most important conclusions to emerge from this comparison are that (i) the new dye is less fluorescent than the parent, (ii) photoisomerization still takes place, despite the presence of a constraining chain, and (iii) the triplet state is formed in low yield. It seems that the decreased fluorescence yield is a consequence of the relatively poor absorption spectral profile, since the excited singlet-state lifetime measured for BLK is slightly longer than that recorded for MC540. Because a relatively



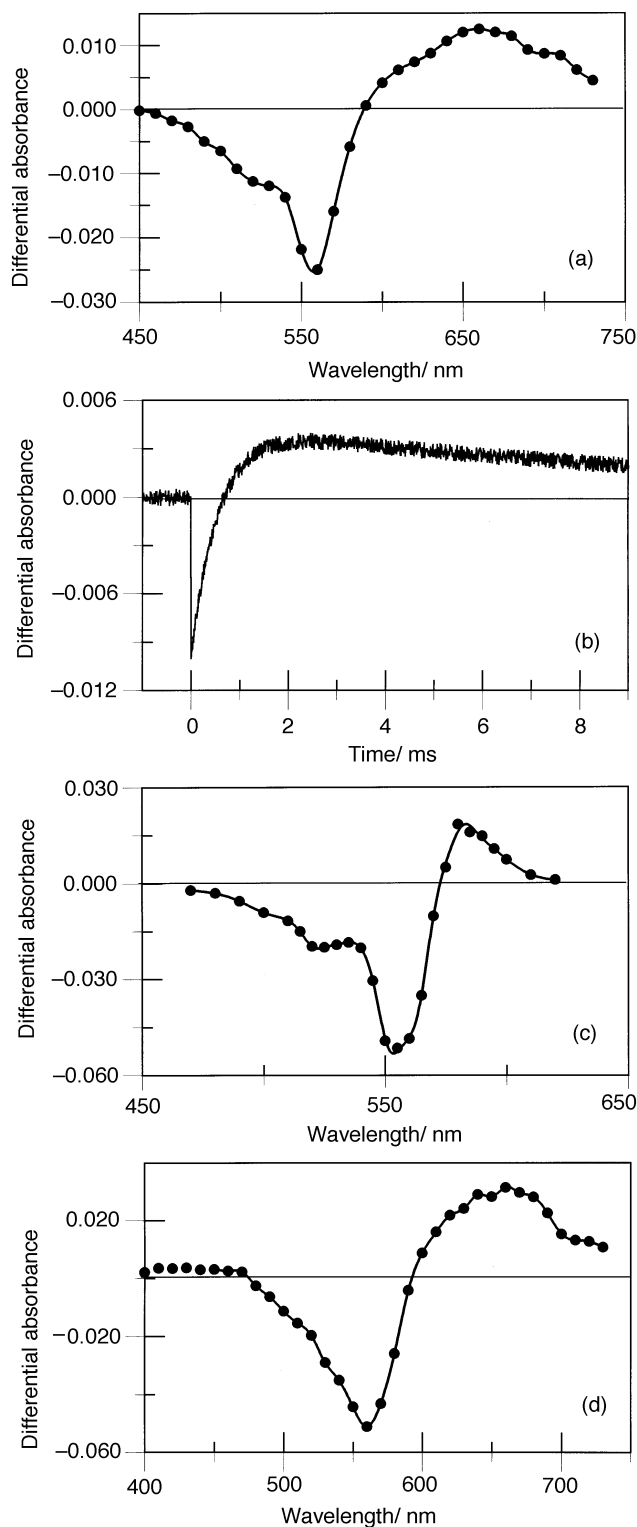


Fig. 5 (a) Differential transient absorption spectrum recorded 20 μ s after excitation of BLK in deoxygenated ethanol solution with a 20 ns laser pulse at 532 nm. (b) Kinetic profile recorded at 575 nm for the above-mentioned experiment, where the shorter-lived triplet excited state shows negative differential absorption and the longer-lived *cis*-isomer shows positive differential absorption. (c) Differential transient absorption spectrum recorded 20 μ s after excitation of BLK in aerated ethanol solution with a 20 ns laser pulse at 532 nm. This spectrum is assigned solely to the formation of the *cis*-isomer. (d) Differential transient absorption spectrum recorded 50 μ s after laser excitation (FWHM = 20 ns, λ = 355 nm) of anthracene in deoxygenated ethanol solution containing BLK (5×10^{-5} mol dm $^{-3}$). This spectrum is attributed solely to the triplet excited state of BLK.

stable isomer is formed upon illumination, it follows that isomerization must occur at the central double bond in the polyene backbone. There is no alternative site. Relative to MC540, the quantum yield and the rate constant ($k_{TS} = \Phi_1/\tau_S$) for formation of the *cis*-isomer are substantially reduced but the rate constant for overall internal conversion ($k_{IC} = (1 - \Phi_F)/\tau_S$) is more comparable. The lifetime of the *cis*-isomer is also somewhat longer for BLK than for MC540. These various findings can be rationalized in terms of isomerization of MC540 occurring at the $C_0=C_1$ double bond while, necessarily, BLK isomerizes at the $C_2=C_3$ double bond.

In this respect, a key observation is that the rate of *cis*-to-*trans* isomerization, being a thermal process, is slower for BLK than for the unconstrained parent dye. The molar volume of the rotor is larger for MC540, regardless of which double bond isomerizes, because of the presence of the water-solubilizing group. Furthermore, steric crowding between the propyl chain and H_{10} causes slight structural distortion for the *cis*-isomer of BLK, as does steric interaction with H_9 in the corresponding *trans*-isomer (Fig. 3). Both these factors should enhance the rate of isomerization for BLK relative to MC540. According to our MO calculations, the bond order at the isomerizing bond (N_{BO}) is similar for both BLK and MC540, while the valence electronic charges (V_{EC}) at C_1 and C_3 in the polyene remain comparable for the two compounds (Table 1). A higher bond order, characterizing increased double-bond character, would decrease the rate of isomerization at that site. Similarly, the valence electronic charge reflects the ability of the polyene bridge to support zwitterionic resonance forms having increased electron density on the bridge. It is seen that the constraining chain exerts little real influence on these properties. Therefore, it becomes difficult to interpret the observation that isomerization is faster in MC540 except in terms of the two compounds undergoing isomerization at different sites that generate perpendicular transition states of quite disparate geometry.

Conclusion

Incorporating the $C_0=C_1$ double bond into a small ring, while preventing isomerization at this site, has not had the desired effect of increasing the fluorescence quantum yield. Two important factors combine to limit the effectiveness of this strategy. The constraining propyl chain causes sufficient structural distortion to seriously perturb the absorption spectrum and thereby to decrease the radiative rate constant. The second problem is that, having blocked isomerization at the first double bond, rotation occurs around the $C_2=C_3$ double bond. Although the yield of the resultant *cis*-isomer is substantially less than found for the parent dye, the rate constant for overall internal conversion remains competitive with both radiative decay and intersystem crossing to the triplet manifold. It appears unlikely that clinically viable merocyanine dyes, even containing a completely locked polyene backbone, will become accessible by this synthetic approach and it will be necessary to prevent isomerization by an alternative methodology.

The relatively slow rates of *trans*-to-*cis* and subsequent *cis*-to-*trans* isomerization found for BLK most likely reflect increased activation barriers for rotation around the $C_2=C_3$ double bond compared with the corresponding $C_0=C_1$ bond. Our MO calculations suggest a slightly higher bond order at the central double bond and, if correct, this would doubtless contribute towards a raised barrier. In turn, the lower yield of *cis*-isomer noted for BLK implies that the transition states for light-induced and thermal isomerization steps possess somewhat different geometries. Relaxation of the transition state approached *via* the first excited-singlet state promotes internal conversion without direct involvement of the *cis*-isomer. This is not so for MC540, where relaxation of the transition state

results in essentially equal probability of forming either isomer.

While it is clear that BLK can isomerize only at the $C_2=C_3$ double bond, there is no compelling experimental evidence to indicate which double bond is more susceptible to isomerization in the unconstrained parent dye. There is little difference in calculated bond order for the $C_0=C_1$ and $C_2=C_3$ double bonds (Table 1) while the increase in rotor volume associated with rotation around the $C_2=C_3$ double bond is <10% of the total. Furthermore, for MC540 there is no stereochemical barrier for rotation around the central double bond. Only a single isomer is apparent in the laser flash photolysis studies but the resultant *cis*-isomer is extremely photolabile. The same is true for the *cis*-isomer formed from BLK and it seems that, in both cases, photolysis of the *cis*-isomer results in formation of the original *trans*-isomer. Experimental studies¹¹ are entirely consistent with isomerization occurring at the $C_0=C_1$ double bond when bulky substituents are added at the C_1 site but do not address the issue of where isomerization takes place in the parent dye. Circumstantial evidence, mostly from kinetic studies, suggests that isomerization in MC540 also takes place at the $C_0=C_1$ double bond, but proof remains elusive. We will attempt to resolve this issue further in future investigations.

This work was supported by the Royal Society of London (A.H.) and the University of Glasgow (A.C.B.). The award of a J.W.T. Jones Travel Fellowship (A.C.B.) is also gratefully acknowledged. The nanosecond laser flash spectroscopic studies were made at the Free Radical Research Facility at the Paterson Institute for Cancer Research (Manchester, UK). Funding for this facility, together with travel costs, is generously provided by the European Commission under the Access to Large-Scale Facilities Scheme. We are especially grateful to the staff of the PICR-FRRF for so readily making available their technical expertise during these investigations.

References

- 1 K. S. Gulliya, *Novel Chemotherapeutic Agents: Preactivation in the Treatment of Cancer and Aids*, R. G. Landes Co., Austin, Texas, 1996.

- 2 F. Sieber, *Photochem. Photobiol.*, 1987, **46**, 1035.
- 3 P. H. Aramendia, M. Krieg, C. Nitsch, E. Bittersman and S. E. Braslavsky, *Photochem. Photobiol.*, 1989, **48**, 187.
- 4 J. Davila, A. Harriman and K. S. Gulliya, *J. Chem. Soc., Chem. Commun.*, 1989, 1215.
- 5 M. Hoebeke, J. Piette and A. Van der Vorst, *J. Photochem. Photobiol. B*, 1991, **9**, 281.
- 6 J. Davila, A. Harriman and K. S. Gulliya, *Photochem. Photobiol.*, 1991, **53**, 1.
- 7 R. W. Redmond, M. B. Srichai, J. M. Bilitz, D. D. Schlomer and M. Krieg, *Photochem. Photobiol.*, 1994, **60**, 348.
- 8 A. Harriman, *J. Photochem. Photobiol.*, 1992, **65**, 79.
- 9 A. C. Benniston, K. S. Gulliya and A. Harriman, *J. Chem. Soc., Faraday Trans.*, 1994, **90**, 953.
- 10 A. C. Benniston, K. S. Gulliya and A. Harriman, *J. Chem. Soc., Faraday Trans.*, 1997, **93**, 2491.
- 11 A. C. Benniston, A. Harriman and C. McAvoy, *J. Chem. Soc., Faraday Trans.*, 1997, **93**, 3653.
- 12 P. R. Dragsten and W. W. Webb, *Biochemistry*, 1978, **17**, 5228.
- 13 N. S. Dixit and R. A. Mackay, *J. Am. Chem. Soc.*, 1983, **105**, 2928.
- 14 A. C. Benniston, A. Harriman and C. McAvoy, *J. Chem. Soc., Faraday Trans.*, 1998, **94**, 159.
- 15 A. C. Benniston and A. Harriman, *J. Chem. Soc., Faraday Trans.*, 1994, **90**, 2627.
- 16 M. M. Romanov, Ju. L. Slominskij, A. L. Tolmachev and F. S. Babichev, *Dopov. Akad. Nauk. Ukr. Ser. B: Geol. Khim. Biol. Nauki.*, 1976, **9**, 807.
- 17 G. Porter and M. W. Windsor, *Discuss. Faraday Soc.*, 1954, **17**, 178.
- 18 I. Carmichael and G. L. Hug, *J. Phys. Chem. Ref. Data*, 1966, **15**, 1.
- 19 L. Pekkarinen and H. Linschitz, *J. Am. Chem. Soc.*, 1960, **82**, 2407.
- 20 J. K. Hurley, N. Sinai and H. Linschitz, *Photochem. Photobiol.*, 1983, **38**, 9.
- 21 L. Pauling, *The Nature of the Chemical Bond*, Cornell, Ithaca, New York, 1960.
- 22 J. B. Birks, *Photophysics of Aromatic Molecules*, Wiley-Interscience, New York, 1970.
- 23 K. S. Gulliya, J. Davila and A. Harriman, *The Cancer J.*, 1990, **3**, 360.
- 24 S. R. Meech and D. Phillips, *J. Photochem.*, 1983, **23**, 193.
- 25 S. J. Strickler and R. A. Berg, *J. Chem. Phys.*, 1962, **37**, 814.

Paper 8/01248B; Received 12th February, 1998